Electronic Structure and Spectra of Linear Dicyano Complexes

W. Roy Mason

*Contribution from the Department of Chemistry, Northern Illinois University,
DeKalb, Illinois 60115. Received December 19, 1972*

Abstract: Electronic absorption and magnetic circular dichroism (MCD) spectral measurements are reported for the linear dicyano complexes of Cu(I), Ag(I), Au(I), and Hg(II). In addition to aqueous and nonaqueous measurements at 300°K, some low-temperature absorption measurements are reported for $Au(CN)_2^-$ and $Ag(CN)_2^-$ in glassy EPA solutions at 77°K and for solid films of $[(n\text{-}C_4H_9)_4N][Au(CN)_2]$ and $[(n\text{-}C_4H_9)_4N][Ag(CN)_2]$ at 40°K. Spectral resolution is markedly enhanced at low temperature, especially for the gold complex for which 27 bands were resolved between 40,000 and 54,000 cm^{-1}. The intense absorptions observed for the $M(CN)_2^-$ complexes are characterized as metal → ligand charge-transfer type from the occupied metal d orbitals to the cyanide π^* level $2\pi_u$. A semidetailed interpretation of the $Au(CN)_2^-$ absorption and MCD spectra is given in terms of an energy level scheme which includes metal spin–orbit coupling. Spectral assignments are also given for $Ag(CN)_2^-$ and $Cu(CN)_2^-$. The results are discussed in terms of d orbital participation in σ bonding and in both π-donor and π-acceptor bonding with the CN$^-$ ligand.

In spite of their simple geometry, relatively little is known about the electronic structures of linear two-coordinate metal complexes.[1,2] Linear two coordination is most prevalent among complexes of metal ions of nd^{10} electronic configuration, although it is not the only structure exhibited by these ions. However, for complexes of Cu(I), Ag(I), Au(I), and Hg(II) with simple ligands, linear two coordination is a common structure.[3] Some complexes of Pt(0), Tl(III), and Cd(II) are also believed to have two-coordinate structures, but evidence indicates that higher coordination in both the solid and solution is important in these cases.[3–7]

In order to provide a basis for a discussion of electronic structures of linear two-coordinate complexes, a systematic investigation of the electronic spectra of some representative complexes has been undertaken. The present paper reports studies on the dicyano complexes of Cu(I), Ag(I), Au(I), and Hg(II). These dicyano complexes are among the most stable and best characterized two-coordinate complexes known, being resistant to solvolysis and, in the case of $Au(CN)_2^-$, to disproportionation. Simple linear structures are indicated from Raman and infrared studies[8–12] of $Ag(CN)_2^-$, $Au(CN)_2^-$, and $Hg(CN)_2$ salts both in solution and in the solid state, from X-ray diffraction of $KAu(CN)_2$[13] and $KAg(CN)_2$,[14] and from neutron diffraction of $Hg(CN)_2$.[15] The structure of the $Cu(CN)_2^-$ ion, however, is not so clear. In solid $KCu(CN)_2$ the Cu(I) is

essentially three-coordinate with two cyano ligands bound through carbon making an angle of 136°, while the nitrogen of a third ligand fills the third position.[6] The structure in solution is not known. Aqueous solution infrared measurements[16] reveal only a single C–N stretching frequency, while solid $KCu(CN)_2$ shows several. While this observation can be interpreted in terms of a bent structure in which the symmetric stretch is quite weak and not observed, it also is consistent with a linear structure.

Previous electronic spectral studies of the $M(CN)_2^-$ ions have been limited to aqueous solution measurements at room temperature.[2,17–20] Detailed interpretation of these spectra is notably lacking, though some assignments have been suggested.[2,19] The present paper reports not only aqueous absorption measurements to 54,000 cm^{-1} but also measurements for $Au(CN)_2^-$ and $Ag(CN)_2^-$ in nonaqueous solvents, including EPA which forms a rigid, transparent glass at 77°K. In addition to 77°K spectra in EPA solutions, some low-temperature (40°K) spectra were obtained from solid films of tetra-n-butylammonium salts of $Au(CN)_2^-$ and $Ag(CN)_2^-$. In both cases an enhancement of resolution resulted. Further, in an effort to characterize excited states, some magnetic circular dichroism (MCD) measurements at 300°K were made on both aqueous and nonaqueous solutions of the dicyanometalates; MCD has recently emerged as a powerful tool for gaining information on degeneracy of excited states.[21] Finally, the absorption and MCD spectra are interpreted in terms of a molecular orbital energy level scheme.

Experimental Section

Preparation of Compounds. Potassium dicyanoaurate(I), K[Au(CN)$_2$], was prepared according to the literature method[22] and was

(1) (a) L. E. Orgel, *J. Chem. Soc.*, 4186 (1958); (b) J. Dunitz and L. E. Orgel, *Advan. Inorg. Chem. Radiochem.*, 2, 25 (1960).

(2) J. R. Perumareddi, A. D. Liehr, and A. W. Adamson, *J. Amer. Chem. Soc.*, 85, 249 (1963).

(3) A. F. Wells, "Structural Inorganic Chemistry," 3rd ed, Oxford University Press, London, 1962.

(4) R. Ugo, *Coord. Chem. Rev.*, 3, 319 (1968).

(5) M. R. Truter and K. W. Rutherford, *J. Chem. Soc.*, 1748 (1962).

(6) J. D. Graybeal and G. L. McKown, *Inorg. Chem.*, 5, 1909 (1966).

(7) F. A. Cotton and G. Wilkinson, "Advanced Inorganic Chemistry," 3rd ed, Interscience, New York, N. Y., 1972.

(8) L. H. Jones, *J. Chem. Phys.*, 26, 1578 (1957).

(9) L. H. Jones, *Spectrochim. Acta*, 19, 1675 (1963).

(10) L. H. Jones, *J. Chem. Phys.*, 27, 468 (1957).

(11) L. H. Jones, *J. Chem. Phys.*, 27, 665 (1957).

(12) L. H. Jones, *Inorg. Chem.*, 2, 777 (1963).

(13) A. Rosenweig and D. T. Cromer, *Acta Crystallogr.*, 12, 709 (1959).

(14) J. L. Hoard, *Z. Kristallogr., Kristallgeometrie, Kristallphys., Kristallchem.*, 84, 231 (1933).

(15) R. C. Seccombe and C. H. L. Kennand, *J. Organometal. Chem.*, 18, 243 (1969).

(16) R. A. Penneman and L. H. Jones, *J. Chem. Phys.*, 24, 293 (1956).

(17) J. Brigando, *Bull. Soc. Chim. Fr.*, 4, 503 (1957).

(18) E. A. Simpson and G. N. Waind, *J. Chem. Soc.*, 1748 (1958).

(19) (a) C. K. Jorgensen, "Absorption Spectra and Chemical Bonding in Complexes," Addison-Wesley, Reading, Mass., 1962, p 198 ff; (b) C. K. Jorgensen, *Advan. Chem. Phys.*, 5, 33 (1963).

(20) M. Erny and R. Lucas, *C. R. Acad. Sci., Ser. B*, 272, 603 (1971).

(21) For an excellent review, see P. N. Schatz and A. J. McCaffery, *Quart. Rev., Chem. Soc.*, 23, 552 (1969).

(22) O. Glemser and H. Sauer, "Handbook of Preparative Inorganic Chemistry," Vol. II, 2nd ed., G. Brauer, Ed., Academic Press, New York, N. Y., 1965, p 1065.
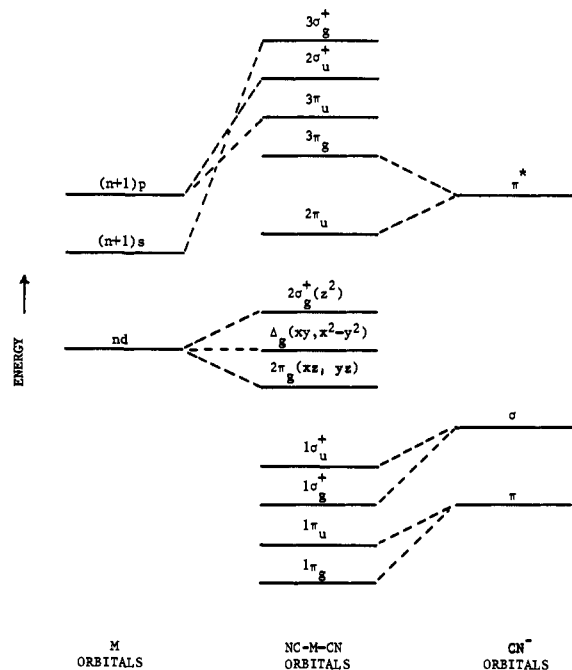
Figure 1. Molecular orbital energy levels for a linear $(D_{\infty h})$ $M(CN)_2{}^{n-}$ complex.

recrystallized twice from hot water. *Anal.* Calcd for K[Au(CN)₂]: C, 8.34; N, 9.72. Found: C, 8.31; N, 9.64. Ir (Nujol, CsI plates): ν_{CN} 2148, ν_{MC} 429 cm⁻¹. The tetra-*n*-butylammonium salt was prepared by precipitation from an aqueous solution with (*n*-C₄H₉)₄NCl. *Anal.* Calcd for [(*n*-C₄H₉)₄N][Au(CN)₂]: Au, 40.08; C, 43.99; H, 7.38; N, 8.55. Found: Au, 39.7; C, 43.76; H, 7.41; N, 8.43. Ir (Nujol, CsI plates): ν_{CN} 2154, ν_{MC} 435 (sh) cm⁻¹.

Potassium dicyanoargentate(I), K[Ag(CN)₂], was prepared by dissolving AgCN in aqueous KCN and crystallizing on a steam bath. The salt was recrystallized twice from hot water. *Anal.* Calcd for K[Ag(CN)₂]: C, 12.07; N, 14.07. Found: C, 11.91; N, 14.02. Ir (Nujol, CsI plates): ν_{CN} 2140, ν_{MC} 394 cm⁻¹. The tetra-*n*-butylammonium salt was precipitated from aqueous solution with (*n*-C₄H₉)₄NCl. The salt forms a hydrate as evidenced by absorption at 1637 and 3400–3600 cm⁻¹ in the infrared. *Anal.* Calcd for [(*n*-C₄H₉)₄N][Ag(CN)₂]·H₂O: C, 51.42; H, 9.10; N, 9.99. Found: C, 51.68; H, 9.22; N, 9.94. Ir (Nujol, CsI plates): ν_{CN} 2143, ν_{MC} 397 cm⁻¹.

Potassium dicyanocuprate(I), K[Cu(CN)₂], was prepared from reagent CuCN and KCN according to the method of Staritzky and Walker.[23] The unrecrystallized salt was washed with water, alcohol, and ether and dried *in vacuo* at room temperature for 24 hr. *Anal.* Calcd for K[Cu(CN)₂]: C, 15.5; N, 18.11. Found: C, 15.5; N, 18.34. Ir (Nujol, CsI plates): ν_{CN} 2091, 2112; ν_{MC} 384, 423 cm⁻¹.

Dicyanomercury(II) was reagent grade and was used without purification. Ir (Nujol, CsI plates): ν_{CN} 2194, ν_{MC} 445 cm⁻¹.

Measurements. All solutions for absorption and MCD spectra were prepared with spectral grade solvents. Concentrations of EPA solutions at 77°K were corrected for solvent contraction using published contraction data.[24] Solid films of [(*n*-C₄H₉)₄N][Au(CN)₂] and [(*n*-C₄H₉)₄N][Ag(CN)₂] were prepared by evaporating concentrated acetonitrile solutions onto quartz (Suprasil) plates. Infrared measurements were made on a Beckman IR12 spectrophotometer. Absorption measurements were made with either a Cary 14 or a Cary 1501 spectrophotometer. For measurements at energies greater than 45,000 cm⁻¹, the Cary 1501 was carefully purged with dry nitrogen. Low-temperature measurements were made with a liquid nitrogen dewar or a Cryotip hydrogen refrigerator (Air Products and Chemicals, Inc.). Magnetic circular dichroism measurements were made with a Durrum-Jasco ORD/UV-5 (with CD attachment) equipped with a permanent magnet. The field strength was 11.0 kG, and the magnet was aligned so that

(23) E. Staritzky and D. I. Walker, *Anal. Chem.*, **28**, 419 (1956).
(24) R. Passerani and I. G. Ross, *J. Sci. Instrum.*, **30**, 274 (1953).

the Verdet constant of water at 595.6 nm was negative. The CD scale was calibrated using optically pure D-[Co(en)₃]I₃ ($\Delta\epsilon = 1.75$ at 489 nm). All MCD measurements were made at 300°K; low-temperature MCD measurements were not possible with our permanent magnet nor were MCD measurements of the solid films because of spurious effects due to strain and linear birefringence in the solid.

Molecular Orbital Energy Levels

A coordinate system for linear dicyano complexes is given in **I**, while metal and ligand orbital basis functions
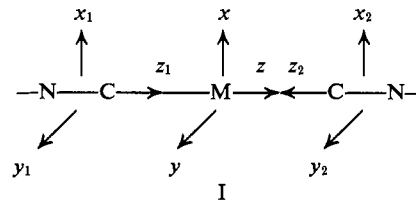
are given in Table I. The $\sigma(i)$, $\pi_z(i)$, and $\pi_y(i)$ functions

Table I. Basis Functions

Symmetry representation	Metal orbitals	Ligand orbital combinations
$\sigma_g{}^+$	nd_{z^2}, $(n+1)s$	$(1/2)^{1/2}[\sigma(1) + \sigma(2)]$
$\sigma_u{}^+$	$(n+1)p_z$	$(1/2)^{1/2}[\sigma(2) - \sigma(1)]$
π_g	nd_{xz}, nd_{yz}	$(1/2)^{1/2}[\pi_x(2) - \pi_x(1)]$ $(1/2)^{1/2}[\pi_x(2) - \pi_y(1)]$
π_u	$(n+1)p_x$, $(n+1)p_y$	$(1/2)^{1/2}[\pi_x(1) + \pi_x(2)]$ $(1/2)^{1/2}[\pi_x(1) + \pi_y(2)]$
Δ_g	$nd_{z^2-y^2}$, nd_{xy}	

represent molecular orbitals of the cyanide ion. A generalized molecular orbital energy level scheme for linear dicyano complexes is presented in Figure 1. Since the complexes under investigation all have d^{10} electronic configuration, the highest filled level is $2\sigma_g{}^+(z^2)$. Consequently the electronic ground state for each complex is nondegenerate and diamagnetic and is designated $^1\Sigma_g{}^+$. Since the coordinates transform as $\sigma_u{}^+(z)$ and $\pi_u(x, y)$ in $D_{\infty h}$, only electronic transitions to $^1\Sigma_u{}^+$ or $^1\Pi_u$ excited states are fully allowed by dipole selection rules in linear molecules. However, in the presence of spin-orbit coupling the spin multiplicity selection rules break down and transitions to formally triplet states may gain appreciable intensity by admixtures of $^1\Sigma_u{}^+$ and $^1\Pi_u$ states.

Results and Discussion

Electronic and Magnetic Circular Dichroism Spectra. Figure 2 presents a comparison of the electronic spectra $Cu(CN)_2{}^-$, $Ag(CN)_2{}^-$, $Au(CN)_2{}^-$, and $Hg(CN)_2$ in aqueous solution to 54,000 cm⁻¹. These spectra are characterized by intense absorption and vary in complexity from the rich spectrum of $Au(CN)_2{}^-$ to the notably empty spectrum of $Hg(CN)_2$. Figures 3 and 4 present spectra obtained at 300 and 40°K from solid films of tetra-*n*-butylammonium salts of $Ag(CN)_2{}^-$ and $Au(CN)_2{}^-$. The low-temperature spectra reveal considerable enhancement of resolution over the aqueous measurements; some 27 bands are observed for $Au(CN)_2{}^-$ between 41,000 and 54,000 cm⁻¹. Similar enhancement was also observed in the low-temperature measurements made on solutions of the tetra-*n*-butylammonium salts in EPA solvent. Detailed spectral
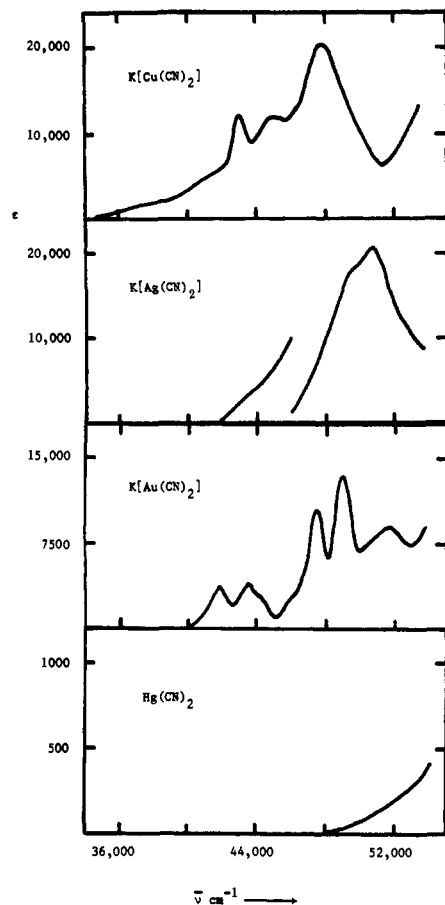
Figure 2. Aqueous solution spectra of the dicyano complexes of Cu(I), Ag(I), Au(I), and Hg(II).

Figure 3. Electronic spectra of [(n-C₄H₉)₄N][Ag(CN)₂] solid film: (———) 300°K, (- - - - - -) 40°K.
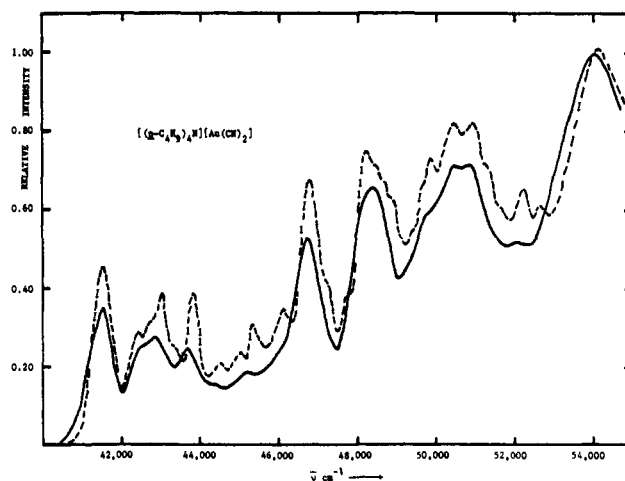
Figure 4. Electronic spectra of [(n-C₄H₉)₄N][Au(CN)₂] solid film: (———) 300°K, (- - - - - -) 40°K.

data for these and other measurements are presented in Table II. It was not possible to obtain low-temperature data for $Cu(CN)_2^-$ since the solubility of the potassium salt in EPA was too low and attempts to convert to the tetra-*n*-butylammonium salt were unsuccessful.

Magnetic circular dichroism spectra for $Cu(CN)_2^-$, $Ag(CN)_2^-$, and $Au(CN)_2^-$ in aqueous solutions are presented along with their absorption spectra in Figures 5, 6, and 7. The MCD of $Hg(CN)_2$ revealed only a gradually increasing negative ellipticity above 45,000 cm⁻¹; no distinct features were noted below 52,000 cm⁻¹.

The MCD spectra for $Au(CN)_2^-$ mirrors the complexity of the absorption spectrum. The numerous features noted in the aqueous MCD measurements were also observed in acetonitrile and EPA solution measurements. Fairly clear positive A terms are observed for the transitions at 47,300 and 48,700 cm⁻¹. In addition a positive A term is associated with the lowest energy band at 41,700 cm⁻¹; however, there is some severe overlapping of terms contributing to the MCD in the region 41,000–46,000 cm⁻¹. Thus it is likely that the disproportionately small positive lobe of the A term at 41,700 cm⁻¹ and the shift of zero ellipticity slightly to 42,000 cm⁻¹ are due to overlap with an adjacent positive A term at 43,300 cm⁻¹. In support of this suggestion a pronounced dip is observed in the MCD spectra near 43,300 cm⁻¹, while an absorbance maximum is observed at nearly the same energy. The MCD between 44,000 and 46,000 cm⁻¹ is complicated
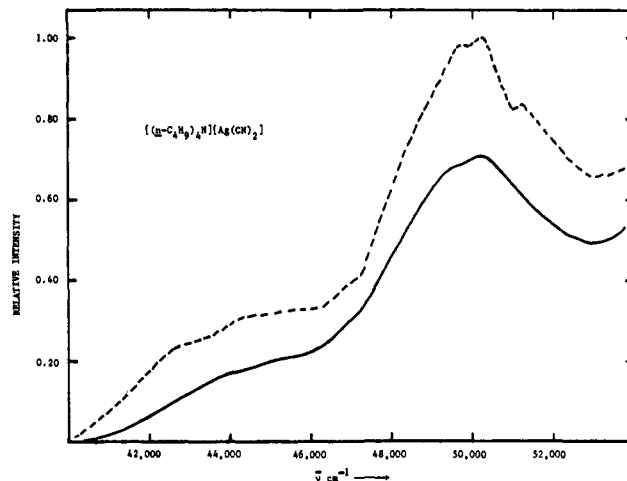
and may consist of overlapping A and B terms. Since the low-temperature absorption spectra reveal numerous weaker bands in this region, it is likely that additional but unresolved features are contributing to the observed MCD.

In aqueous solution the MCD spectra for $Ag(CN)_2^-$ shows a positive B term associated with the weak shoulder at 44,000 cm⁻¹ and a positive A term at 50,000 cm⁻¹. However, there is considerable broadening on the low-energy side of the A term between 46,000 and 49,000 cm⁻¹ suggesting additional unresolved terms.

The MCD spectra for $Cu(CN)_2^-$ in aqueous solution also appears to consist of overlapping terms. The nearly zero ellipticity at 42,900 cm⁻¹ corresponding to an absorption maximum may indicate the presence of a positive A term adjacent to the fairly clear positive A term at 45,300 cm⁻¹. Above 46,000 cm⁻¹ negative B terms are observed at 48,000 and 49,700 cm⁻¹. No absorption band is observed near 49,700 cm⁻¹ but the high-energy side of the absorption maxima at 47,800 cm⁻¹ is rather broad and could hide other transitions.

Spectral Assignments. Except for some weak absorption below 46,000 cm⁻¹ for $Ag(CN)_2^-$ and below 40,000 cm⁻¹ for $Cu(CN)_2^-$, the spectra of the dicyanometalates

Table II. Electronic Spectral Data[a]

| Solid film[b] | | H_2O[c] | CH_3CN | EPA solution | |
300°K	40°K			300°K	77°K
[(n-C4H9)4N][Au(CN2)]					
41.56 (0.350)	41.58 (0.458)	41.74 (3490)	41.75 (4170)	41.62 (4250)	41.75 (5500)
42.46 (0.251)[d]	42.46 (0.293)				
42.85 (0.288)	42.75 (0.321)[d]				
	43.01 (0.387)	43.69 (3740)	43.01 (3810)	43.06 (3680)	
	43.30 (0.250)				42.94 (5060)
					43.29 (4070)[d]
43.67 (0.252)	43.79 (0.391)	44.33 (2410)[d]	43.76 (3680)	43.91 (2370)[d]	44.27 (3500)
44.50 (0.141)	44.58 (0.211)				
	45.04 (0.239)				45.04 (1580)
45.20 (0.192)	45.33 (0.309)		45.35 (2040)	45.64 (1630)[d]	45.82 (2900)
46.00 (0.240)[d]	46.13 (0.349)				
46.68 (0.531)	46.75 (0.675)	47.39 (10,600)	46.95 (8240)	47.06 (10,400)	47.21 (~16,000)
	47.17 (0.420)[d]				
	47.70 (0.383)[d]				
	48.20 (0.745)	49.00 (13,200)	48.54 (12,800)		
48.33 (0.658)	48.38 (0.713)[d]				
	48.55 (0.673)[d]				
	48.80 (0.633)[d]				
	49.40 (0.550)[d]				
	49.60 (0.655)[d]				
49.80 (0.595)	49.86 (0.728)				
50.40 (0.709)	50.45 (0.820)				
50.82 (0.715)	50.90 (0.822)	50.85 (11,000)	51.20 (15,300)		
	51.28 (0.707)[d]				
	51.60 (0.612)[d]				
52.10 (0.523)	52.19 (0.657)	51.71 (9280)[d]			
	52.61 (0.613)				
54.00 (1.000)	54.00 (1.000)				
[(n-C4H9)4N][Ag(CN)2]					
	42.60 (0.233)[d]			42.19 (60)[d]	42.92 (1700)
44.00 (0.242)[d]	44.20 (0.301)[d]	44.00 (450)[d]	44.40 (232)[d]	44.64 (314)[d]	44.35 (780)[d]
45.50 (0.290)[d]	45.60 (0.326)[d]				
	46.90 (0.386)[d]			46.30 (695)[d]	46.40 (1150)
	48.50 (0.761)[d]				47.62 (2260)[d]
49.40 (0.952)[d]	49.60 (0.977)[d]	49.80 (18,500)	49.75 (25,200)[d]		48.31 (~3400)
50.20 (1.000)	50.20 (1.0000)	50.70 (21,000)	50.89 (30,100)		
	51.20 (0.837)				

| K[Cu(CN)2] | | | |
H_2O	CH_3CN	$Hg(CN)_2$	
	35.00 (56)[d]	No Maxima or shoulders below 55,000 cm⁻¹ in water;	
37.70 (1400)[d]	38.00 (330)[d]	a faint fluorescence noted at about 49,000 cm⁻¹ in water	
	40.50 (3900)[d]		
41.20 (5800)[d]	41.50 (8900)[d]		
42.90 (11,500)	42.65 (11,300)		
45.00 (11,000)	44.50 (8500)[d]		
47.80 (21,000)	47.00 (23,000)		

[a] $\tilde{\nu} \times 10^{-3}$ cm⁻¹ (ϵ l. mol⁻¹ cm⁻¹). [b] Prepared from evaporation of CH_3CN solution onto a quartz plate; value in parentheses indicates relative intensity. [c] Potassium salt. [d] Shoulder (ϵ is for the values of $\tilde{\nu}$ given).

are characterized by absorptivities of 1000 or more and are thus reasonably attributed to Laporte-allowed charge-transfer transitions from the $^1\Sigma_g^+$ ground state to ungerade excited states. The temperature dependence of the spectra observed both in the solid films and in EPA solutions for $Au(CN)_2^-$ is consistent with this assignment; the bands tend to sharpen and increase in maximum absorptivity at low temperature. Further, the lowest energy transition for $Hg(CN)_2$ lies at least 15,000 cm⁻¹ higher in energy than the lowest energy transition in the isoelectronic $Au(CN)_2^-$ complex. A blue shift of this type as the oxidation state of the metal is increased is a characteristic of a metal → ligand (M → L) charge transfer. Therefore, the logical assignment of the absorption in these complexes is charge transfer from the filled metal d orbitals to the empty ligand-based $2\pi_u$ orbital. Transitions of the M → L type to $3\pi_g$, even if present at energies accessable to measurement, are expected to be weak and therefore

obscured by the intense absorption. The possibility of transitions from the metal d orbitals to $3\pi_u$ or $2\sigma_u^+$ which are derived from metal p orbitals is considered unlikely since these levels will certainly be of too high energy. The free ion $nd - (n + 1)p$ energy separations from atomic spectral data[25] vary from about 60,000 cm⁻¹ in Au(I) and Cu(I) to more than 80,000 cm⁻¹ in Ag(I). Participation of the p orbitals in bonding is expected to increase this separation even further.

$Au(CN)_2^-$. By far the best resolved spectral data were obtained for the $Au(CN)_2^-$ ion. Consequently a more detailed interpretation is possible in this case than for the $Ag(CN)_2^-$ or $Cu(CN)_2^-$ ions, and much of the present discussion will deal with the gold complex.

The marked difference in complexity between the $Au(CN)_2^-$ spectra and that of $Ag(CN)_2^-$ is striking, both from the number of individual bands resolved and

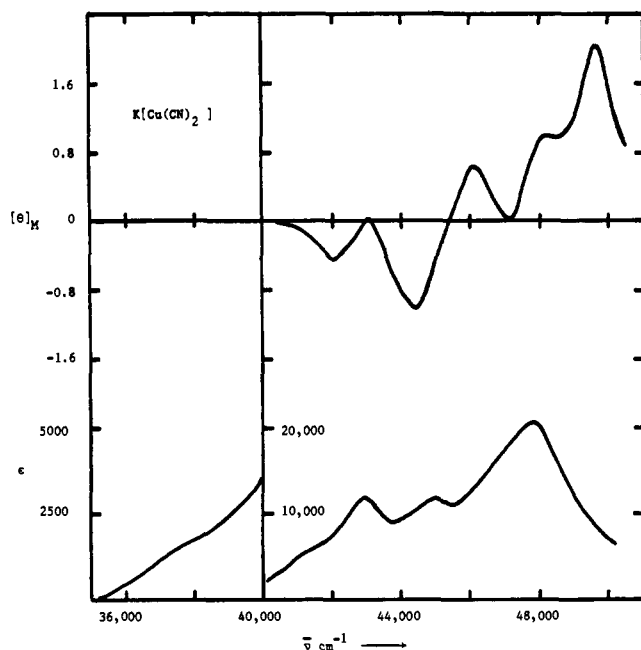(25) C. E. Moore, Nat. Bur. Stand. (U. S.) Circ., No. 467, 2 (1952); 3 (1958).

Figure 5. Electronic (lower curves) and MCD (upper curves) spectra of K[Cu(CN)$_2$] in H$_2$O.
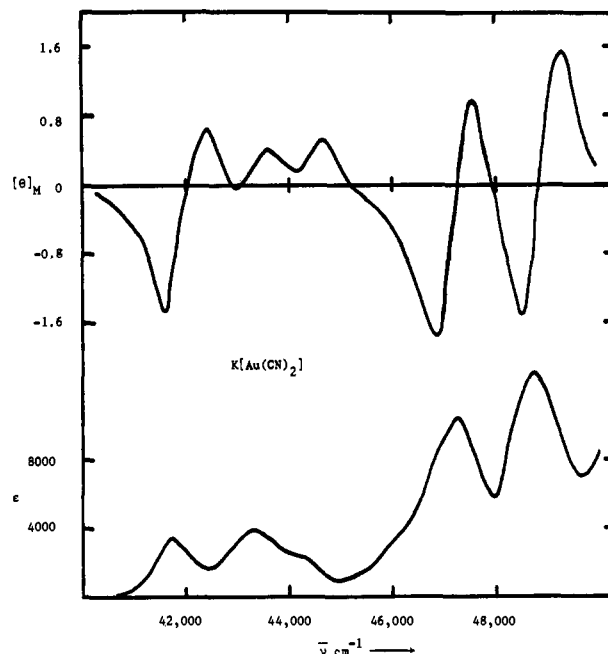

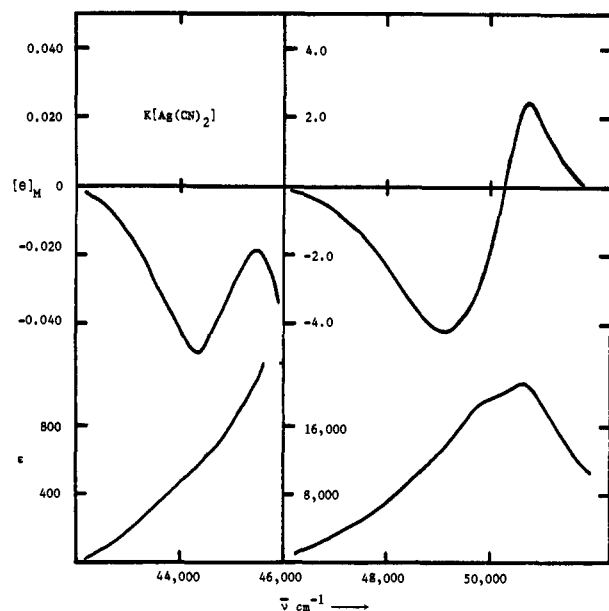Figure 7. Electronic (lower curve) and MCD (upper curve) spectra of K[Au(CN)$_2$] in H$_2$O.

Figure 6. Electronic (lower curves) and MCD (upper curves) spectra of K[Ag(CN)$_2$] in H$_2$O.

Figure 8. Excited states for nd → 2π_u (cyanide) excitations.

from the higher intensity of the lowest energy bands in the gold complex. This difference may be offered as an indication of the greater importance of metal spin–orbit coupling interaction in the Au(I) complex since spin–orbit effects will give rise to excited-state energy splitting and allow spin-forbidden transitions to gain intensity. The difference between the metal spin–orbit coupling constants for silver and gold is substantial; the constants for Ag(I) and Au(I) free ions are respectively $\zeta_{4d} = 1830$ and $\zeta_{5d} = 5100$ cm^{-1}.[26] Spin–orbit effects from the ligands can be ignored since the coupling constants for carbon and nitrogen of cyanide are very much smaller than the metal.

(26) J. S. Griffith, "Theory of Transition Metal Ions," Cambridge University Press, Cambridge, 1964, Appendix 6.
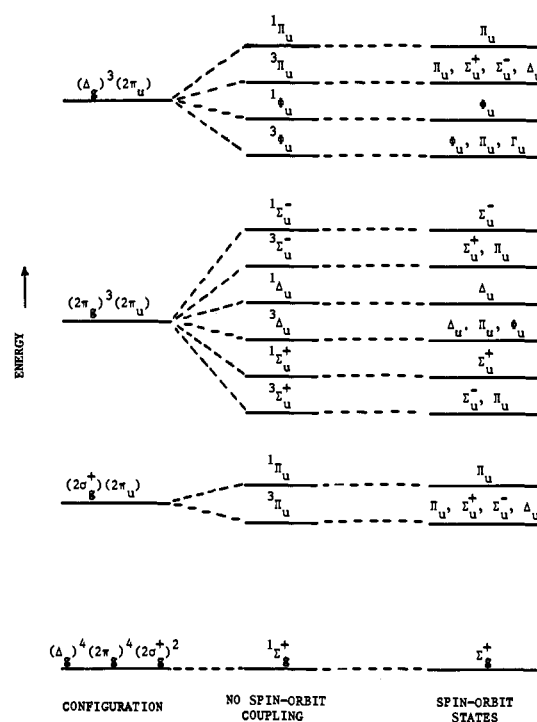
The approach taken to treating the problem of spin–orbit interaction in the interpretation of the Au(CN)$_2$$^-$ spectra has been to consider spin–orbit coupling as a perturbation on the excited states expected for M → L charge transfer in the absence of strong coupling. Figure 8 shows the possible excited states for the d → 2π_u excitations 2$\sigma_g$$^+$($z^2$) → 2$\pi_u$, 2$\pi_g$($xz$, yz) → 2π_u, and Δ_g(xy, $x^2 - y^2$) → 2π_u neglecting spin–orbit coupling and the double group states on inclusion of strong spin–orbit coupling. The double group excited states are characterized by the lack of spin multiplicity superscripts. Twenty-four excited states arise from the

Mason / *Electronic Structure and Spectra of Linear Dicyano Complexes*

three d $\rightarrow$ $2\pi_u$ excitations in the presence of spin–orbit coupling. Input data for the spin–orbit problem included estimated energies for the unperturbed singlet and triplet excited states assumed in the absence of spin–orbit coupling and a value of the spin–orbit parameter ζ. A suitable secular determinant was diagonalized to find the energies of the spin–orbit states, which were then compared to experimental spectra. The most intense bands in the spectra are expected to involve transitions to Σ_u^+ or Π_u states. Transitions to Δ_u, Φ_u, and Γ_u states are symmetry forbidden and are expected to be weaker. Consequently only the Σ_u^+ and Π_u states were treated in the spin–orbit calculations.

As an example or the spin–orbit treatment consider the eight Π_u states in Figure 8. Each Π_u state is described by a wave function of the form in eq 1. The

$$|\Pi_u(i)\rangle = a_i|\Pi_u(a^1\Pi_u)\rangle + b_i|\Pi_u(a^3\Pi_u)\rangle +$$
$$c_i|\Pi_u(^3\Sigma_u^+)\rangle + d_i|\Pi_u(^3\Delta_u)\rangle + e_i|\Pi_u(^3\Sigma_u^-)\rangle +$$
$$f_i|\Pi_u(^3\Phi_u)\rangle + g_i|\Pi_u(b^3\Pi_u)\rangle + h_i|\Pi(b^1\Pi_u)\rangle \quad (1)$$

energies of these Π_u states as well as the coefficients of each eigenvector are determined by diagonalizing the appropriate 8×8 Hermitian secular determinant, the upper triangle of which is given in eq 2. The Q_i in

Table III. Spin–Orbit Σ_u^+ and Π_u States for Au(CN)$_2^-$

Calcd spin–orbit states,[a] cm^{-1}		Absorption spectra,[b] cm^{-1}	Obsd MCD term[b]
$\Pi_u(2)$	41.72	41.74	$+A$
$\Sigma_u^+(1)$	44.74	43.69	$+A^e$
$\Pi_u(6)$	45.09	44.33	e
$\Pi_u(1)$	47.39[c]	47.39	$+A$
$\Sigma_u^+(4)$	47.52		
$\Pi_u(7)$	49.01	49.00	$+A$
$\Pi_u(3)$	50.92	50.86	
$\Sigma_u^+(2)$	51.71	51.71	
$\Pi_u(4)$	52.32		
$\Pi_u(8)$	53.36		
$\Sigma_u^+(3)$	54.30	54.00[d]	
$\Pi_u(5)$	58.34		

[a] Calculated for $\zeta = 2750$ cm^{-1}; $Q_1(\Pi_u) = Q_2(\Pi_u) = 47{,}390$ cm^{-1}; $Q_3(\Pi_u) = Q_4(\Pi_u) = Q_5(\Pi_u) = 52{,}000$ cm^{-1}; $Q_6(\Pi_u) = Q_7(\Pi_u) = Q_8(\Pi_u) = 49{,}100$ cm^{-1}; $Q_1(\Sigma_u^+) = 46{,}500$ cm^{-1}; $Q_2(\Sigma_u^+) = Q_3(\Sigma_u)^+ = 51{,}500$ cm^{-1}; $Q_4(\Sigma_u^+) = 48{,}500$ cm^{-1}. [b] Aqueous solution. [c] Calculations scaled to fit the 47,390-cm^{-1} band in the absorption spectrum. [d] Observed in the solid film spectra at 300°K. [e] Uncertain due to overlapping terms.

The approach here has been one of obtaining a reasonable set of parameters Q_i and ζ which will place spin–orbit states at energies that agree favorably with experimental spectra and then to test this set of parameters for uniqueness. Choices of Q_i and ζ were guided

$$\begin{bmatrix} -E + Q_1 & 0 & \frac{3^{1/2}}{2}i\zeta & \frac{3^{1/2}}{2}i\zeta & \frac{3^{1/2}}{2}i\zeta & 0 & 0 & 0 \\ & -E + Q_2 & \frac{-3^{1/2}}{2}i\zeta & \frac{-3^{1/2}}{2}i\zeta & \frac{-3^{1/2}}{2}i\zeta & 0 & 0 & 0 \\ & & -E + Q_3 & \frac{-i}{2}\zeta & \frac{-i}{2}\zeta & \frac{i}{2}\zeta & \frac{i}{2}\zeta & \frac{-i}{2}\zeta \\ & & & -E + Q_4 & \frac{-i}{2}\zeta & \frac{i}{2}\zeta & \frac{i}{2}\zeta & \frac{-i}{2}\zeta \\ & & & & -E + Q_5 & \frac{i}{2}\zeta & \frac{i}{2}\zeta & \frac{-i}{2}\zeta \\ & & & & & -E + Q_6 & i\zeta & i\zeta \\ & & & & & & -E + Q_7 & i\zeta \\ & & & & & & & -E + Q_8 \end{bmatrix} = 0 \quad (2)$$

eq 2 are the energies of the unperturbed singlet and triplet states. The spin–orbit matrix elements are calculated assuming the molecular orbitals derived from the metal d orbitals are approximated by metal d functions. The spin–orbit matrix elements then reduce to matrix elements of angular momentum between the d orbitals. A similar set of wave functions, eq 3, and

$$|\Sigma_u^+(i)\rangle = a_i|\Sigma_u^+(a^3\Pi_u)\rangle + b_i|\Sigma_u^+(^1\Sigma_u^+)\rangle +$$
$$c_i|\Sigma_u^+(^3\Sigma_u^-)\rangle + d_i|\Sigma_u^+(b^3\Pi_u)\rangle \quad (3)$$

a 4×4 secular determinant, eq 4, can be written for

$$\begin{bmatrix} -E + Q_1 & (3/8)^{1/2}i\zeta & (3/8)^{1/2}i\zeta & 0 \\ & -E + Q_2 & -(i/2)\zeta & -(i/2)\zeta \\ & & -E + Q_3 & 0 \\ & & & -E + Q_4 \end{bmatrix} = 0 \quad (4)$$

the four $\Sigma_u^+(i)$ states.

by the MCD data since the observation of an A term is consistent only with a Π_u state.

Table III presents calculated energies for the Σ_u^+ and Π_u spin–orbit states along with the energies of absorption bands and MCD terms observed in aqueous solution for comparison. Table IV presents the mixing coefficients for the spin–orbit eigenvectors determined for the input parameters of Table III. A wide range of parameters was tried, but values of the Q_i and ζ significantly different from those given in Table III failed to produce a favorable spectral fit and in addition place Π_u states near the 41,740, 47,390, and 49,000 cm^{-1} bands. This latter point is significant since MCD terms are quite clearly observed for these three bands. Further, each of these A terms is positive. If only one-centered integrals are included, the $2\pi_u$ orbital is approximated by a carbon 2p function, and the metal orbitals are assumed to be 5d functions, one can write an approximate expression for the predicted A terms.[27,28]

(27) S. B. Piepho, P. N. Schatz, and A. J. McCaffery, J. Amer. Chem. Soc., 91, 5994 (1969).

Table IV. Mixing Coefficients for Spin–Orbit States of Au(CN)₂⁻ᵃ

State	a	b	c	d	e	f	g	h
				Πᵤ States				
Πᵤ(1)	0.707	0.707	0	0	0	0	0	0
Πᵤ(2)	0.400	−0.400	−0.093	−0.008	0.078	0.347	−0.257	0.268
	+0.010i	−0.010i	+0.311i	+0.325i	+0.316i	−0.008i	−0.234i	−0.221i
Πᵤ(3)	−0.188	−0.188	−0.506	−0.060	0.539	−0.118	0.032	−0.060
	−0.024i	−0.024i	−0.196i	+0.539i	−0.637i	−0.115i	+0.115i	+0.103i
Πᵤ(4)	−0.095	−0.095	−0.499	0.431	−0.271	−0.124	−0.228	0.189
	−0.163i	−0.163i	+0.030i	−0.252i	+0.420i	−0.211i	+0.088i	+0.155i
Πᵤ(5)	−0.147	−0.147	0.447	0.382	0.248	0.149	−0.004	−0.254
	+0.234i	0.234i	+0.061i	+0.240i	+0.377i	−0.237i	−0.280i	+0.117i
Πᵤ(6)	0.391	−0.391	−0.060	−0.010	0.041	0.460	0.132	−0.199
	+0.030i	−0.030i	+0.118i	+0.132i	+0.126i	+0.036i	+0.442i	+0.416i
Πᵤ(7)	−0.147	0.147	−0.041	−0.012	0.025	0.541	−0.550	0.531
	−0.041i	−0.041i	+0.019i	+0.044i	+0.038i	+0.149i	−0.116i	+0.183i
Πᵤ(8)	0.067	−0.067	−0.227	0.292	0.175	0.257	0.436	0.238
	+0.098i	−0.098i	−0.273i	−0.202i	+0.309i	+0.366i	−0.089i	−0.376i
				Σᵤ⁺ States				
Σᵤ⁺(1)	0.879	−0.075	0.080	0.056i				
	−0.006i	+0.326i	+0.325i					
Σᵤ⁺(2)	−0.258	−0.205	0.601	−0.242				
	+0.181i	+0.565i		−0.345i				
Σᵤ⁺(3)	−0.221	0.650	0.128	0.144				
	−0.246i	+0.060i	+0.640i	+0.130i				
Σᵤ⁺(4)	0.015	0.065	−0.007	0.878				
	+0.133i	+0.309i	−0.316i	−0.101i				

ᵃ Determined for the input parameters of Table III.

This expression is given in eq 5 where β is the Bohr

$$A_i \cong \frac{\beta}{2}[|a_i|^2 + |b_i|^2 + 2|c_i|^2 + 2|d_i|^2 + 2|e_i|^2 +$$

$$5|f_i|^2 + 3|g_i|^2 + 3|h_i|^2]D_{\Pi u}(|a_i|^2 + |h_i|^2) \quad (5)$$

magneton, $D_{\Pi u}$ is the dipole strength of a $^1\Sigma_g^+ \rightarrow$ $^1\Pi_u$ transition which is fully allowed, and a_i-h_i are the coefficients of the Π_u eigenvectors. Thus the observed positive A terms are consistent with this crude approximation. In view of the approximations, the magnitudes of the A terms are considered substantially less reliable than the overall sign and, therefore, will not be discussed further.

Although the results of the calculations are encouraging, the parameter magnitudes necessary require some discussion. First of all, the value of the spin-orbit parameter $\zeta = 2750$ cm⁻¹ is only 54% of the free ion spin-orbit coupling constant. Attempts to use larger values of ζ, and hence a smaller reduction in spin-orbit coupling from the free ion values, were unsatisfactory. For example, ζ in the range of 4000–5000 cm⁻¹ predicted a Π_u state below 40,000 cm⁻¹ which would give rise to a transition of easily measurable intensity. No bands of absorptivity greater than 0.1 were observed below 40,000 cm⁻¹. Thus, the results of the calculations suggest that there is substantial reduction of spin-orbit coupling in the complex compared to the free ion. Such a reduction may at first seem too large, being much larger than the reduction usually observed in complexes of the 3d transition elements (~80–85% of free ion values). However, reductions of ~50% or below have been observed in other complexes involving the 5d transition elements. For example, reductions of from 30 to 47% of free ion values have been found for several octahedral fluoride complexes MF₆ (M = Os(VI), Ir(VI), and Pt(VI)) of the

5d transition metals.[29] The spin-orbit coupling constant is proportional to the square of the effective charge on the central metal, Z_*^2.[19,30] It is generally believed that considerable charge reduction occurs for heavy metal complexes chiefly through covalency of the metal ligand bonds. In the present case the reduction of charge on the gold is likely to involve the utilization of 6s and 6p orbitals rather than extensive involvement of the 5d orbitals (see discussion below). The 6s and 6p₂ orbitals strongly penetrate the 5d orbitals, and therefore electron density from the ligands will reduce the effective charge felt by 5d electrons, thus lowering the effective 5d spin-orbit coupling constant.

A second point which is noteworthy is that reduction of effective charge Z_* also lowers interelectronic repulsions as evidenced by reduction of the Racah parameters B and C in transition metal complexes compared to the free ions. As in the case of the spin-orbit parameters (though the data are not as extensive for 5d complexes compared to 3d or 4d complexes), a *greater* reduction in $B_{complex}$ and $C_{complex}$ is observed for 5d complexes.[19,30] Therefore, fairly low interelectronic repulsions are in keeping with the small differences in energies of the unperturbed singlet and triplet states suggested by the successful input parameters. In addition only small energy differences between singlet and triplet states of the same symmetry type are expected for the states involved in M → L charge transfer since the states differ only in the spin of the two electrons, and the occupied and empty orbitals are quite different spatially.[31]

Finally, the values of Q_i parameters provide qualitative information concerning the placement of the one-electron d molecular orbital energy levels. Since differences in interelectronic repulsions are expected to

(28) P. N. Schatz, A. J. McCaffery, W. Suëtaka, G. N. Henning, A. B. Richie, and P. J. Stephens, *J. Chem. Phys.*, 45, 722 (1966).

(29) W. Moffitt, G. L. Goodman, M. Fred, and B. Weinstock, *Mol. Phys.*, 2, 109 (1959).

(30) C. K. Jorgensen, *Struct. Bonding (Berlin)*, 1, 3 (1966).

(31) H. B. Gray and C. D. Cowman, private communication, 1971.

be small, the Q_i parameters indicate the one-electron energy level ordering is probably $2\sigma_g^+(z^2) > \Delta_g(x^2 - y^2, xy) > 2\pi_g(xz, yz)$. This ordering differs from the order predicted from electrostatic (crystal field) calculations: $\sigma_g^+ > \pi_g > \Delta_g$.[32] However, the placement of $2\pi_g(xz, yz)$ lowest in energy is consistent with d orbital participation in M $\rightarrow$ L back-donation; such back-donation would stabilize the $2\pi_g(xz, yz)$ level and destabilize $3\pi_g$ from the cyanide. In support of M $\rightarrow$ L back-donation involving the d orbitals, Jones has pointed out[12] that the integrated intensity of the antisymmetric ν_{CN} in a variety of cyanide complexes parallels the degree of π back-donation, with higher intensities being associated with back-donation. In this connection the integrated intensity of ν_{CN} for $Au(CN)_2^-$ is considerably higher than for $Hg(CN)_2$, and Jones has suggested that this observation is consistent with a higher degree of back-donation in the Au(I) complex compared to Hg(II)—a suggestion which is not at all unreasonable in view of the lower charge on the gold which is thus expected to have more expanded 5d orbitals than mercury.

In addition to the more intense features assigned to Σ_u^+ or Π_u spin–orbit states, the solid film spectra reveal a number of poorly resolved shoulders on the intense bands near 48,000 and 50,000 cm^{-1} and some weaker bands between 42,000 and 47,000 cm^{-1} and between 52,000 and 53,000 cm^{-1}. Some regularity in band spacing in the region of the 48,000 and 50,000 cm^{-1} bands is noted and may be offered as evidence for vibrational structure. The average spacing between four adjacent bands in the former is $\sim$190 cm^{-1} and between seven adjacent bands in the latter is $\sim$370 cm^{-1}. Vibrational progressions are expected only for the symmetric modes of the complex since electronic transitions involved are to unsymmetric (u) excited states. From analysis of Raman spectra,[9,10] the symmetric modes have been assigned as $\nu_{CN}(\Sigma_g^+) = 2164$ cm^{-1}, $\nu_{MC}(\Sigma_g^+) = 452$ cm^{-1}, and $\delta_{MCN}(\Pi_g) = 305$ cm^{-1}. Therefore the structure in the region of the 50,000-cm^{-1} band may involve ν_{MC}, while the structure associated with the 48,000-cm^{-1} band may be due to the M–C–N bending mode. The structure is unfortunately too poorly resolved to be absolutely confident of these assignments, however, and the series of bands observed in both regions may be due to individual electronic transitions.

The weaker bands between 42,000 and 47,000 cm^{-1} and between 52,000 and 53,000 cm^{-1} show no definite progressions and therefore are likely due to symmetry-forbidden transitions to Δ_u, Γ_u, or Φ_u excited states. Such transitions could gain intensity by excited-state distortion (Jahn–Teller) of the linear complex to C_{2v} symmetry, which would lift the degeneracy of the Δ_u, Γ_u, and Φ_u states. Transitions to Σ_u^- states are expected to be weak regardless of excited-state distortions from linearity.

Ag(CN)$_2^-$ and Cu(CN)$_2^-$. Spectral assignments for Ag(CN)$_2^-$ and Cu(CN)$_2^-$ are less definitive because of the poorer resolution and the relatively small number of features to provide a basis for interpretation. Some spin–orbit calculations for Ag(CN)$_2^-$ were attempted, but the results were inconclusive—the problem being

(32) R. Krishnamurthy and W. B. Schaap, *J. Chem. Educ.*, 46, 799 (1969).

one of more parameters than observables. The observation of a positive A term for the broad complex band at 50,000 cm^{-1} suggests transitions to one or more Π_u states, probably the formally spin-allowed ones arising from the $2\sigma_g^+(z^2) \rightarrow 2\pi_u$ and $\Delta_g(x^2 - y^2, xy) \rightarrow 2\pi_u$ excitations. The lower energy side of the MCD A term is quite broad and may hide B terms for Σ_u^+ states. The lower intensity bands between 42,000 and 48,000 cm^{-1} are also poorly resolved even at low temperature. The logical assignment for this absorption is to symmetry forbidden transitions to Δ_u, Γ_u, and Φ_u states and weaker formally spin-forbidden transitions to Σ_u^+ and Π_u states. A detailed assignment must await better resolved spectra.

The question of the solution structure of $Cu(CN)_2^-$ is not answered by the present electronic spectral measurements. The observation of an MCD A term could be offered as evidence for degeneracy indicating a linear structure in solution since the bent structure would not have any strictly degenerate levels. However, the sensitivity of the energy levels to the degree of bending of the complex is not known, and a "pseudo" A term could result from two closely spaced but formally nondegenerate levels. It appears that the electronic spectra can be interpreted in terms of a linear structure or one that is only "slightly bent."

Three intense bands at 42,900, 45,000, and 47,800 cm^{-1} are prominent in the $Cu(CN)_2^-$ spectrum.[20] These are assigned to transitions to the formally spin-allowed $\Pi_u[2\sigma_g^+(z^2) \rightarrow 2\pi_u]$, $\Pi_u[\Delta_g(x^2 - y^2, xy \rightarrow 2\pi_u]$, and $\Sigma_u^+[2\pi_g(xy, yz) \rightarrow 2\pi_u]$ states, respectively. The positive MCD A terms visualized at 42,900 and 45,000 cm^{-1} are consistent with these assignments. As a consequence of these assignments, the ordering of the one-electron d molecular orbitals is likely similar to that postulated for the gold complex, *viz.*, $2\sigma_g^+(z^2) > \Delta_g(x^2 - y^2, xy) > 2\pi_g(xz, yz)$, though it must be admitted that differences in electron repulsions, which would be greater for Cu(I), could change the ordering. The weaker shoulder observed at 41,200 cm^{-1} is probably due to symmetry forbidden or formally spin-forbidden transitions. The origin of the absorption below 40,000 cm^{-1} is unclear and may be due to impurities in the $Cu(CN)_2^-$ sample. Some calculations of the spin–orbit energies of Σ_u^+ and Π_u states indicate that if the 42,900-cm^{-1} band is due to the lowest energy formally spin-allowed transition, all other Σ_u^+ or Π_u states would lie above 40,000 cm^{-1}. It is probable that Δ_u, Γ_u, and Φ_u states would also lie above 40,000 cm^{-1}. Complexes such as $Cu(CN)_4^{3-}$ or $Cu(CN)_3^{2-}$ are known to have bands below 40,000 cm^{-1}, however.[18,20]

Bonding in the Dicyanometalates. From electrostatic arguments, Orgel[1] and others[7] have concluded that linear two coordination in d^{10} metal complexes is the result of strong d–s mixing on the central metal, rather than to special stability of sp hybrid orbitals. This conclusion was based on comparisons of the nd, $(n + 1)$s, and $(n + 1)$p orbital energies in Hg^{2+}, Au$^+$, Ag$^+$, and Cu$^+$ ions with orbital energies in neighboring metal ions which are prone to have higher coordination numbers; the metal ions which form two-coordinate complexes are characterized by comparatively small d–s energy separations. Thus, according to this argument, considerable d-orbital participation in σ bonding would be expected. However, the results

of the present study are inconsistent with this view for the dicyano complexes.

Ignoring differences in interelectronic repulsions, which are expected to be relatively small, the comparatively small energy differences in the Q_i parameters for $Au(CN)_2^-$ (and $Cu(CN)_2^-$) indicate that the σ-bonding $2\sigma_g^+(z^2)$ and π-bonding $2\pi_g(xz, yz)$ levels are very close in energy to the nonbonding $\Delta_g(x^2 - y^2, xy)$ level. The total energy splitting of the one-electron d levels is likely less than 5000–7000 cm^{-1}. As Figure 9 shows this is in marked contrast to the d-orbital energy splitting in d^8 square-planar tetracyanometalate complexes between the empty σ-bonding $b_{1g}(x^2 - y^2)$ and the occupied π-bonding $b_{2g}(xy)$ and $e_g(xz, yz)$ and σ-bonding $a_{1g}(z^2)$ levels; the splitting is estimated to be between 30,000 cm^{-1} for $Ni(CN)_4^{2-}$ and >50,000 cm^{-1} for $Pt(CN)_4^{2-}$.[33] Undoubtedly, the more effective use of the empty $d_{x^2-y^2}$ orbital for σ bonding is responsible for the very much larger splitting in $M(CN)_4^{n-}$ compared to $M(CN)_2^-$; the effects due to π bonding are substantially smaller and appear to be comparable in both cases. Thus, there is a marked reduction in the utilization of the d orbitals for σ bonding on adding a pair of electrons to the metal on going from d^8 to d^{10}. This is not altogether unexpected though since the d σ orbitals in question are *antibonding* and occupation will result in electronic destabilization. Instead there must be a shift in orbital utilization to the $(n + 1)$s and $(n + 1)p_z$ for σ bonding. Support for 6s and 6p orbital participation in σ bonding is available from some recent Mössbauer measurements on $KAu(CN)_2$[34] and other gold(I) compounds.[35] The Mössbauer of KAu-$(CN)_2$ is characterized by a very large isomer shift and quadrupole splitting, the former interpreted in terms of 6s orbital contributions and the latter in terms of $6p_z$ orbital involvement.[34]

The utilization of the metal d orbitals for π bonding in the dicyanometalates is more difficult to assess since the cyanide ligand possesses both filled π and empty π^* orbitals which can be involved in bonding. Ligand → metal ($L_\pi \to M$) donor bonding will surely destabilize the $2\pi_g(xz, yz)$ level, but metal → ligand ($M \to L_{\pi^*}$) will be stabilizing. The ultimate placement of the $2\pi_g(xz, yz)$ level is dependent upon both types of interaction. The results of fitting the spectra for Au-$(CN)_2^-$ (and $Cu(CN)_2^-$) suggest that the $2\pi_g(xz, yz)$

Figure 9. A comparison of d orbital energy splitting in planar d^8 $M(CN)_4^{n-}$ and linear d^{10} $M(CN)_2^{n-}$ complexes. The energy ordering and approximate separations for the $M(CN)_4^{n-}$ complexes are from ref 33; see text.

level is very nearly nonbonding. It is noteworthy though that both effects, $L_\pi \to M$ and $M \to L_{\pi^*}$, will serve to increase the metal–ligand binding. Consistent with this view, the dicyanometalates are known to be very stable complexes[16,36] and likely have very strong M–C bonds. Perhaps a useful way of visualizing the two kinds of π interaction is to consider the effects to be *synergic*. Thus $M \to L_{\pi^*}$ back-donation would tend to make $L_\pi \to M$ donation more favorable. The net result would be an increase in M–C bond order at the expense of C–N bond order.[37]

In addition to $L_\pi \to M$ bonding involving the d orbitals, it is probable that the $(n + 1)p_z$ and $(n + 1)p_y$ metal orbitals play an important role. In fact, the reluctance of the nd^{10} metal ions of low oxidation state to expand their coordination numbers may be due to relatively stable metal p orbitals. Expansion of coordination, while perhaps energetically justifiable in terms of σ bonding, will of necessity require a sacrifice of $L_\pi \to M$ bonding using metal p orbitals.

(33) W. R. Mason and H. B. Gray, *J. Amer. Chem. Soc.*, **90**, 5721 (1968).

(34) M. O. Faltens and D. A. Shirley, *J. Chem. Phys.*, **53**, 4249 (1970); D. A. Shirley, *Science*, **161**, 745 (1968).

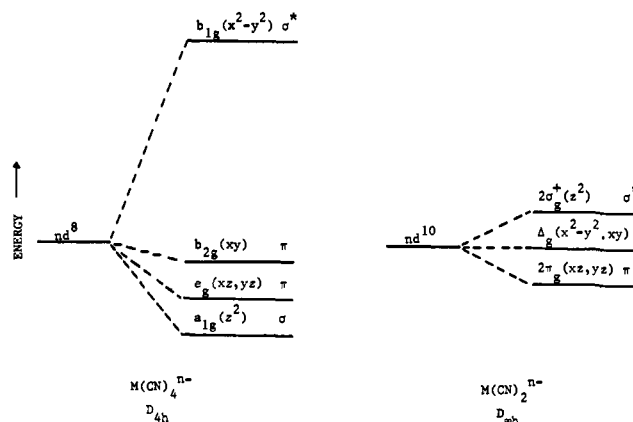(35) J. S. Charlton and D. I. Nichols, *J. Chem. Soc.*, 1484 (1970).

(36) See, for example, B. M. Chadwick and A. G. Sharpe, *Advan. Inorg. Chem. Radiochem.*, **6**, 83 (1966).

(37) Although both $L_\pi \to M$ and $M \to L_{\pi^*}$ bonding would be expected to reduce the C–N bond order, and therefore reduce the C–N stretching frequency, the measured values of ν_{CN} for all of the dicyano complexes are *higher* than for the free ligand. σ bonding will also affect ν_{CN}, however. Fenske and DeKock[38] have recently pointed out that the 5σ donor orbital of CN$^-$ is slightly *antibonding* with respect to the C–N σ bond, so that strong σ donation by the cyano ligand is expected to raise ν_{CN} relative to that of the free ligand. Thus, little can be inferred about the M–C bonding from the energy of ν_{CN}.

(38) R. F. Fenske and R. L. DeKock, *Inorg. Chem.*, **11**, 437 (1972).